diffusion-fundamentals
The Open-Access Journal for the Basic Principles of Diffusion Theory, Experiment and Application

# Diffusion: Macroscale Dwarf and Nanoscale Giant

*Nikolaus Nestle*[1]

[1] BASF Aktiengesellschaft, Ludwigshafen, Germany

Corresponding author:
Nikolaus Nestle
BASF AG Ludwigshafen
GKP/P, G201
D-67056 Ludwigshafen
E-Mail: nikolaus.nestle@basf.com

**Abstract**

Diffusion processes of particles or energy exhibit a characteristic scaling behavior with space and time. In this contribution, the background of this scaling behavior will be shortly described and its consequences in physics, chemistry, biology and various areas of technology shall be explored. Furthermore, some demonstration experiments for different aspects of diffusion and its scaling behavior will be discussed in the course of the article.

Keywords: Diffusion, scaling-behaviour, chemical technology, food science, demonstration experiments

## 1. Introduction and a short look into usual demonstration experiments

A standard demonstration of diffusion processes in German experimental physics lectures involves a large (up to 1 m high) glass cylinder the lower part of which is filled with a blue, concentrated solution of copper sulfate which then is carefully overlaid with colourless demineralized water. If done by a skilful experimentalist, the interface between both solutions is initially quite sharp (with a transition zone of maybe 1 to 2 millimeters and with the density difference between the water and the solution additionally stabilizing the original stratification. Over the course of a two-hour lecture, one can already recognize some widening of the interface region due to interdiffusion of blue copper ions (and their colorless sulfate counterions) into the demineralized water region. The interface zone may grow to about 1 to 2 cm in this time. In some places, especially in the State of Saxony, the cylinder is then carefully positioned into a wooden rack and kept on public display for the remaining term or even longer (see fig. 1). There is even a special name for this rack with the cylinders in it: It is called “Semesteruhr”, i.e. “term clock”. This name illustrates quite well that major changes in the distribution of the copper ions over the cylinder may take several terms, coming close to equilibration even years.

The appearance of a “term clock” a few weeks after filling perfectly represents the typical perception of diffusion on the macroscale: It may lead to some blurring of formerly sharp interfaces, but is slow and it does not reach very far, and in order to



Diffusion Fundamentals 6 (2007) 1.1 - 1.24


Fig. 1: "Term clock" at the University of Leipzig grand physics lecture theatre, spring 2000.

prevent it, one must carefully pay attention to avoid other more effective mixing processes such as convection. However, the initial hours of the experiment provide already some clue that this may not be the complete picture: In this phase of the experiment, a notable change in the interface region between copper sulfate solution and free water can be observed as a matter of one or two hours. This suggests that diffusion may initially be "faster" than at later stages.

Not working inside academia right now and therefore lacking the means to set up a real "term clock" for closer inspection of the initial hours of the process, I was looking for a simpler demonstration experiment for interdiffusion in order to provide some experiment-based illustrations for this article. Searching on internet, I first bumped into the suggestion to use just a few crystallites of potassium permanganate in a small water-filled dish. The example pictures coming along with the experiment description looked quite similar to those shown in fig. 2. Indeed one can see "diffuse" color fronts inside the dish, however the asymmetric appearance of the colored region clearly indicates some asymmetry which should not be observable for a purely diffusive process.

Fig. 2: Some $KMnO_4$ crystallites in a slightly tilted water-filled plate (directly after application and ca. 5 min later).

Furthermore, we see the $KMnO_4$ venturing away from the crystallite to distances much bigger than one should expect on the basis of the mean diffusive shift of water (1.2 mm using eq. 2.12 assuming $D = 2.3\times10^{-9}\mathrm{m}^2/\mathrm{s}$). Actually, the propagation of the dissolved permanganate ions is strongly affected by density-driven flow (the density of $KMnO_4$ solution is higher than that of water). Only in the longer run diffusion effects will soften up the concentration gradient between the heavy $KMnO_4$ solution creeping along the bottom of the dish and the lighter overstanding water. The dominating role of density-driven flow is not just unique for the dissolution of $KMnO_4$ but happens in a similar way for other water-

soluble substances. It can be suppressed by adding appropriate thickening agents to the water. Some bacterial exopolysaccharide materials are known to have only a minor impact on the diffusion behaviour of water and dissolved molecules while at the same time dramatically increasing the viscosity of the water (see section 4.4) By adding such agents to the water, we can suppress density-driven flow processes almost completely while not affecting the diffusion too much. Fig. 3 shows some snapshots from an experiment performed with eosin ($C_{20}H_6Br_4Na_2O_5$) as a dye in a dish filled just with water and the other with a watery solution of 0.3 g/l xanthan gum [1] as a thickening agent. (Doing the experiment with $KMnO_4$ is not possible as xanthan gum and similar thickeners chemically react with $KMnO_4$.) As can be seen from the figure, the purely diffusive transport of eosin in the xanthan-doped water is orders of magnitude slower than the density-driven flow in the pure water.

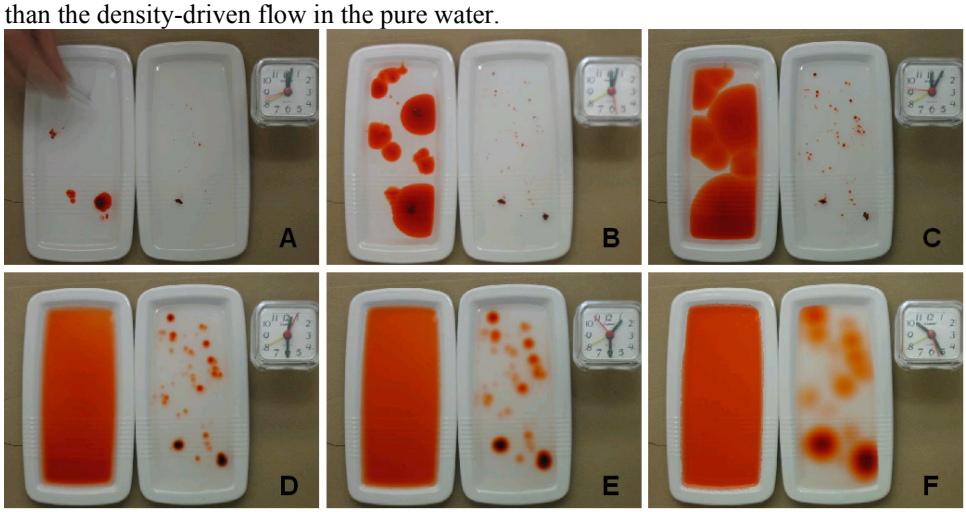


Fig. 3: Distribution of dissolving eosin in a water-filled dish (left) and a dish with 0.3 % xanthan gum solution (right): In the water-filled dish, the eosin has already covered a substantial part of the dish while the crystallites are still applied (A, B). After 5 min, more than half of the dish is occupied by the eosin solution while the propagation of the eosin in the xanthan gum solution is just about 1 mm (C). After 30 min, the eosin in the xanthan gum solution has propagated by a few mm while the eosin in the water is homogeneously distributed (D). After 90 min, the eosin in the xanthan gum has spread around each crystallite by about 5 mm (E), and after 625 min the diffusive spread is about 15 mm (F). Note also the different intensities of the individual eosin spots which are due to different amounts of eosin in the original crystallites.

As the gravity-driven flow tends to stabilize the interface between two miscible liquid phases of different density, it can be used to prepare a demonstration experiment for purely diffusive transport: Fig. 4 shows a water-filled vial where an intensively coloured, sugar-containing syrup was injected locally near the bottom. As can be seen from the figure, this procedure leads, after a few minutes, to a sharp and flat interface between the syrup and the water – a perfect starting point for a 1D diffusion experiment. Some snapshots of this are given in the figure. For a semiquantitative observation of the diffusion process, a simple digital camera with remote control from a PC or a long-term

serial image function is sufficient. Alternatively, the experiment can be run completely qualitatively with stuff completely available at any bar.


Fig. 4: Diffusive mixing between a lower layer of sweet red fruit syrup and the overstanding water. A: directly after the injection of the lingonberry syrup, B: about 6 h later, C: about 12 h later and D: about 24 h later.

Again, the pictures in fig. 4 show the characteristic behavior with the diffusive broadening of the interface front starting quite fast and becoming subsequently slower.

The length scale of the experiment in figure 4 is a few mm, and the time scale is on the order of hours, and the slowing down on a time scale of days is obvious. So this again fits very well with the idea of diffusion on macroscopic scales being a slow process.

Looking back at the density-driven flow of $KMnO_4$ and eosin in water, we get an indication that diffusion on short length scales must be a much more effective process: In order to feed the long-range propagation by the density driven flow, the molecules from the dissolving crystallites must first diffuse through an almost stagnant laminary liquid layer at the surface of the crystallite. Obviously the diffusive flow through this layer must be quite fast as it can sustain the fast long-range flow of considerable amounts of material.

Common to all the diffusion experiments described up to now is the observation of a particle current against a concentration gradient in absence of any other driving force except this gradient. Furthermore, all those processes were instationary diffusion processes: Due to the diffusive current, the concentration gradient itself is beginning to smoothen out. In a stationary diffusion process, by contrast, the concentration gradient against which the diffusion is occurring remains constant.

Visualizing a stationary diffusion process in condensed matter experimentally is rather difficult [2]. A macroscopic scale experiment in liquid phase is additionally complicated by the fact that the stationary diffusion will be preceded by a long period of instationary diffusion until a concentration equilibrium is reached in the diffusion bridge between the two reservoirs of constant concentration. Therefore, it is typically not demonstrated in lecture hall experiments.

As diffusion of energy is much faster than diffusive material in condensed matter, it is much easier to demonstrate stationary diffusion of energy instead of matter. The diffusion of energy is more commonly known as “heat conduction”. The analog to the concentration of a substance in the heat diffusion experiment is the temperature. An everyday example of (almost) stationary heat conduction is the temperature gradient along a wall between a heated (or chilled) building and the outside world (see fig. 5). Demonstrating stationary heat diffusion experimentally is much easier, and a heat current can for example be determined by the evaporation losses of a liquid phase or by electronic heat flow meters. Alternatively, the temperature gradient along the heat bridge

may be observed via thermochromic dyes, multisite temperature sampling with thermoelements or thermographic imaging via IR cameras.

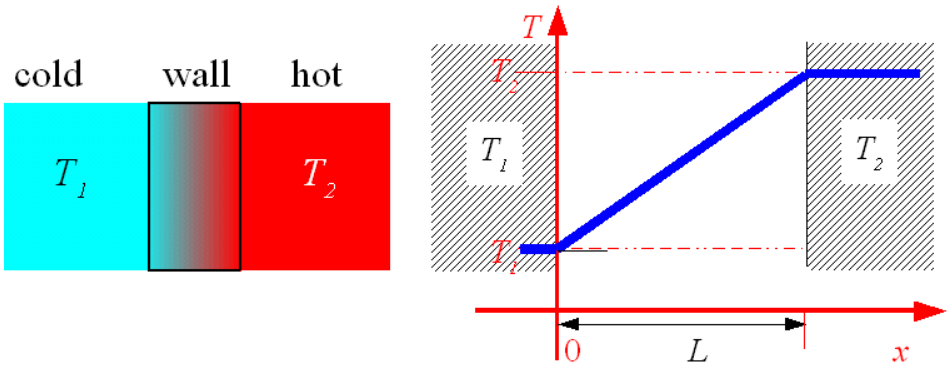


Fig. 5: Stationary heat diffusion and temperature profile through a wall separating a cold and a hot reservoir (e.g. the air-conditioned inside of a house from the hot outside).

## 2. From the labtable to the blackboard: Fick's laws and a phenomenological description of diffusion

### *2.1 Stationary diffusion and Fick's first law*

The phenomenological description of stationary diffusion is given by Fick's first law which is also known as Fourier's law in the context of heat diffusion (actually, Fick developed his phenomenological description of diffusion on the basis of Fourier's work on heat conduction [2]). It relates the diffusive current $j_D$ to the concentration gradient:

$$j_D = -D\frac{\mathrm{d}c}{\mathrm{d}x} \text{ in the 1D case,} \qquad (2.1)$$

$$\vec{j}_D = -D\nabla c \text{ in the 3D case, respectively.} \qquad (2.2)$$

Fourier's law is written completely analog and relates the heat current $j_Q$ to the concentration gradient :

$$j_Q = -\lambda\frac{\mathrm{d}T}{\mathrm{d}x} \text{ in the 1D case,} \qquad (2.3)$$

$$\vec{j}_Q = -\lambda\nabla T \text{ in the 3D case, respectively.} \qquad (2.4)$$

The diffusion coefficient $D$ and the heat conductivity $\lambda$ are scalar material constants in the standard textbook treatment of these transport phenomena. In anisotropic materials, this is not any more the case, and a diffusion or heat conductivity tensor is needed to describe the transport properties of the materials. Anisotropic diffusion properties are quite common in biological systems, anisotropic heat conduction is typical for anisotropically structured materials of biological or technical origin (e.g. wood: about 1.8 times higher thermal conductivity in fiber direction [3]).

*2.2 Instationary diffusion and Fick's second law*

In the description of instationary diffusion, we will consider the diffusion balance inside a given differential element under the assumption that Fick's first law is valid on differential time and length scales. For the sake of simplicity, we will provide the detailed calculation just for the 1D diffusion case.

If we consider the concentration change d$c$ in a volume element d$x$ localized at the site $x$ during the time d$t$ we find on the basis of a simple material balance for the concentration change:

$$\frac{\mathrm{d}c}{\mathrm{d}t}\mathrm{d}x = \left(j_D(x) - j_D(x+\mathrm{d}x)\right)$$

i.e. the difference between inflow and outflow leads to a corresponding concentration change. This equation can be rewritten as

$$\frac{\mathrm{d}c}{\mathrm{d}t} = \frac{\left(j_D(x) - j_D(x+\mathrm{d}x)\right)}{\mathrm{d}x}$$

and inserting Fick's law for the diffusion current, we arrive at

$$\frac{\mathrm{d}c}{\mathrm{d}t} = \frac{-D\left(\dfrac{\mathrm{d}c(x)}{\mathrm{d}x} - \dfrac{\mathrm{d}c(x+\mathrm{d}x)}{\mathrm{d}x}\right)}{\mathrm{d}x} = D\frac{\mathrm{d}^2 c}{\mathrm{d}x^2}. \qquad (2.5)$$

The same argument in 3D leads to

$$\frac{\mathrm{d}c}{\mathrm{d}t} = D\Delta c \qquad (2.6)$$

and in heat conduction to

$$\frac{\mathrm{d}T}{\mathrm{d}t} = \frac{\lambda}{C}\Delta T = \alpha\Delta T \qquad (2.7)$$

with $C$ denoting the heat capacity of the material and $\alpha = \frac{\lambda}{C}$ being known under the terms "temperature conductivity" or "heat diffusion coefficient".

Despite their innocent looks which are quite similar to a wave equation

$$\frac{\partial^2 u}{\partial t^2} = {c_p}^2 \Delta u \qquad (2.8)$$

or Schrödinger's equation

$$\frac{\partial \psi}{\partial t} = -\frac{i\hbar}{2m}\Delta\psi \qquad (2.9)$$

equations (2.5) to (2.7) prove mathematically and numerically quite hard to treat, and whole books [4,5] have been devoted to their solution, and it has been only very recently that solutions of the diffusion equation have been incorporated into the repertoire of computer algebra programs such as Maple or Mathematica. Only some good-natured special cases are easier to solve. One of them is the stationary case (i.e. $dc/dt = 0$). This

corresponds to Poisson's equation which leads to the well-known linear concentration or temperature gradient in the 1D case.

The most simple case of an instationary solution of the diffusion equation is the spreading of an "instantaneous" or Delta-source which results in a Gaussian of increasing width

$$w(t) = \sqrt{2Dt} \tag{2.10}$$

and decreasing amplitude:

$$c(x,t) =) \frac{C}{2\sqrt{\pi Dt}} \exp(-\frac{x^2}{4Dt}) \tag{2.11}$$

In addition to the purely theoretical case of the "instantaneous" source, this solution is also valid for a Gaussian initial concentration profile of the width $w$ (which is equivalent to a shift in the starting time by $t_o = \frac{w^2}{2D}$). Other initial concentration profiles such as a step-function will lead to mathematically more complicated concentration profiles involving error functions or series of error functions [5].

The corresponding solutions in the 3D case are

$$w_{3D}(t) = \sqrt{6Dt} \tag{2.12}$$

and

$$c(x,y,z,t) =) \frac{C}{8(\sqrt{\pi Dt})^3} \exp(-\frac{(x^2+y^2+z^2)}{4Dt}) \tag{2.13}$$

*2.3 The "velocity" of diffusive transport*

The common feature of all these solutions in the 1D case is that the width of the diffuse concentration profile will increase according to a square-root-of-time law as in the simple Gaussian case. This square-root-of-time behavior is the reason for the perceived slowdown of diffusive transport over macroscopic distances: Calculating a "velocity" $v_D$ from the mean diffusive shift over a length scale $L = \sqrt{2Dt_L}$, we arrive at

$$v_D = \frac{L}{t_L} = \frac{L}{\frac{L^2}{2D}} = \frac{2D}{L}, \tag{2.14}$$

i.e. the "velocity" of diffusive transport is inversely proportional to the length scale $L$!

The ratio between velocities of directed movement (flow, advection) and the "velocity" of diffusive transport in a system is often characterized by the Péclet number Pe which was initially introduced in the analysis of heat transfer [6].

The Péclet number Pe for diffusion is given as the ratio

$$\mathbf{Pe} = \frac{Lv}{D}, \tag{2.15}$$

for heat transfer as $\mathbf{Pe} = \frac{Lv}{\alpha}$. (2.16)

In the macroscopic world, Péclet numbers tend to be very high, i.e. directed transport processes tend to be much faster than diffusive processes. The propagation of permanganate ions by gravity-driven flow in figure 2 is an example.

On the microscale, by contrast, we find many processes taking place at very low Péclet numbers. The tendency to lower Péclet numbers at short length scales is not only due to smaller values for $L$ but also due to the decreasing flow velocities in smaller structures (at constant pressure difference essentially proportional to $1/L^2$). In the further course of this contribution, we will explore the consequences of this phenomenon in natural and technical systems. But before doing so, we will take a very short look at the molecular mechanism of diffusion and the idea of self-diffusion.

## 3. Diffusion in statistical mechanics, self-diffusion

### *3.1 The statistical picture of diffusion*

The description of diffusion provided by Fick's law is phenomenological and continuous, and quantities like concentrations and temperature are average quantities that become meaningless on the molecular length scale. In order to understand the nature of diffusion on the sub-nm scale, one therefore has to resort to statistical mechanics. First statistical calculations on diffusion in gases were made by James Clerk Maxwell [7] in 1867. A more general statistical description of diffusion processes by statistical mechanics was suggested in 1905 independently by Albert Einstein [8] and Marian von Smoluchowski [9].

In the statistical picture, each molecule is undergoing a random walk which leads to a mean square displacement increasing linear with time – which in turn gives rise to the square-root-of-time behaviour already discussed in the last chapter. If different species of molecules are non-uniformely distributed over a system (which is an unlikely stage in the absence of barriers corralling the molecules in their uneven distribution), we will see a leveling off of these concentration gradients resulting from the random walks of all molecules together: The system moves from an unlikely stage with concentration gradients to a more likely stage with a stochastically uniform distribution of each species of molecules. The change into this more likely stage leads to an increase in the entropy of the system, and it is obvious that this interdiffusion process is irreversible.

While changes in the local chemical composition of the system and increases in entropy only take place in the case of interdiffusion processes along concentration gradients, the molecular motions leading to each molecule's random walk are also there in thermal equilibrium.

### *3.2 Experimental approaches to self-diffusion*

Due to the indistinguishable nature of molecules, this self-diffusion process cannot be observed directly without manipulations trying to mark individual molecules. The classical way to mark the molecules is the use of (radioactive or stable) isotope tracers: If

the usually tiny differences between molecules containing different isotopes are neglected, following the changing distribution of the isotope tracer in the system provides an experimental access to the self-diffusion process in the system. A key player in developing the radiotracer approach to diffusion studies was von Hevesy [10] who developed the radiotracer approach both for studies of self-diffusion and interdiffusion processes. Other experimental approaches to self-diffusion studies are quasielastic neutron scattering (where essentially the momentum transfer between individual molecules and an incident neutron beam is probed) and nuclear magnetic resonance (which allows the transient encoding of position information onto the nuclear spins by appropriate manipulations of their precession phase in field gradient NMR [11,12] or by selective excitation of very thin slices [13]).

Special features of field gradient NMR are the options of working at well-defined diffusion times [14,12] and well-defined diffusive shift lengths [15]. With such experimental options available, field gradient NMR allows the study of porous systems from the perspective of the molecules diffusing in them. Depending on the diffusion coefficient of the liquid phase and its NMR behavior inside the porous material of interest, the diffusion length scales accessible in the experiments may range from a few 10 nm to several 100 μm. The dependence of the measured diffusion coefficient on diffusion times and/or reciprocal shift vectors therefore provides unique information on the internal structure of the material's pore system. The field-gradient NMR experiment is non-destructive and can be continuously repeated. Like that, it is also possible to study changes in the structure and transport properties of a developing pore system such as a hydrating cement stone matrix [16]. NMR effects are not only sensitive to the well-defined magnetic field gradients used in field gradient NMR but also to statistical gradients present in many micro-and nano-structured materials [17,18]. The way how internal magnetic field variations inside a sample manifest themselves in its NMR behavior is dependent on the ratio of the mean diffusive shift during the time scale of the NMR experiment and the length scale of the magnetic field variation inside the sample: If the length scale of the variation is much bigger than that of diffusion, a distribution of well-defined NMR frequencies can be observed. If the diffusion length scale is larger than the length scale of field variation, it manifests itself mainly by a characteristic attenuation of the NMR signals. This difference in the NMR behavior is the result of the decreasing effectiveness of diffusive mixing processes: if the length scale of the magnetic field gradients is comparable or shorter than the mean diffusive shift during the NMR time scale, each diffusing molecule experiences its own stochastic averaging of NMR frequencies. This in turn leads to the macroscopic attenuation of the NMR signal. If the time scale of an NMR experiment is varied, the joint action of diffusion and NMR can be different, too (see fig. 6).

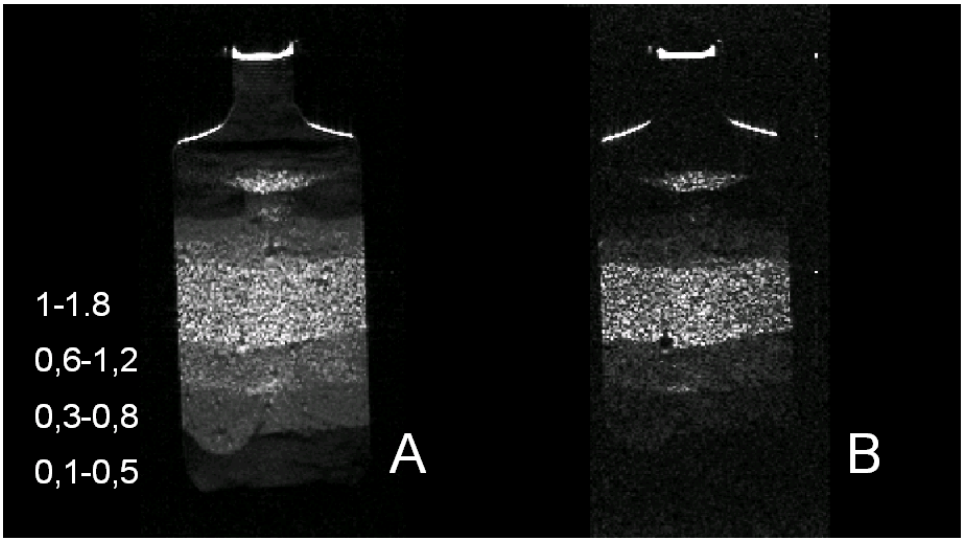


Fig. 6: NMR signal attenuation due to diffusion in internal magnetic field gradients: turbo spin echo MRI scan (A; echo time: 96 ms, 7 refocussing pulses during echo time) and spin echo MRI scan (B; echo time 96 ms, no refocusing during echo time) of a bottle filled with water and sand layers of different grain size (written in mm next to image A). The stronger echo attenuation in the fine-grained sand layers near the ends of the bottle in image B is due to diffusion effects in the internal magnetic field gradients produced by the sand grains.

## 4. Diffusive transport in technical and natural systems; the role of geometry

### *4.1 Diffusion limited reactions with a migrating reaction zone; the Stefan model*

In the absence of convective processes, any reaction in an extended medium needs diffusive transport between an external reservoir and the reaction zone (see fig. 7). The same holds true for transport of heat to a phase transition zone. If the reaction process is sufficiently fast and irreversible, we can assume that the reactant is used up as soon as it meets unreacted material. In this case, it can be shown that the reaction zone travels into the medium according to the following relation [19,5,20] in the 1D case:

$$x(t) = \sqrt{\frac{2Dc_{res}t}{c_{bind}}} \qquad (4.1)$$

with $c_{bind}$ denoting the concentration of available binding sites in the material and $c_{res}$ denoting the concentration of the reactant in the reservoir.

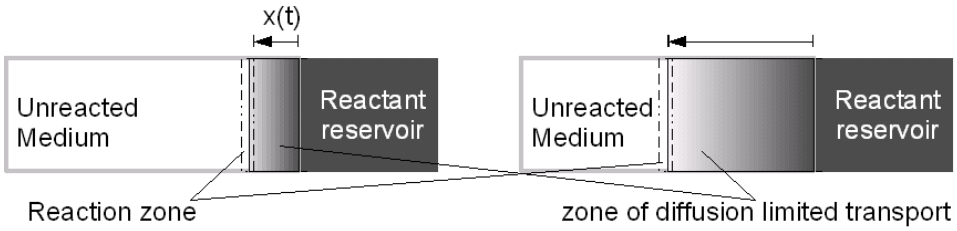


Fig. 7: Reaction front propagating by purely diffusive transport into an extended medium: With increasing intrusion of the front into the medium, the zone of diffusion limited transport becomes wider. This in turn leads to an increasing diffusion resistance which has to be overcome by the reactant.

The same model can be applied for the migration of a phase transition zone [19]. Both the reaction zone in this case and the mean square displacement in the case of pure diffusion propagate according to a square-root of time-law into the medium. The difference between the two cases is the shape of the intruding front: in the Stefan case, the concentration profile goes to exactly 0 after the reaction zone while the concentration profile in the purely diffusive case exhibits a Gaussian "tail" extending far into the medium. It should be noted that the diffusion length may actually be longer than the intrusion depth of the reaction front into the medium [21].

The reaction rate in a Stefan-type process is limited by the diffusive current between the reservoir and the reaction zone and therefore decreases like the "velocity" of a pure diffusion process (see eqn. 2.14) with increasing intrusion depth $x(t)$ of the reaction front:

$$\frac{\mathrm{d}N_{prod}}{\mathrm{d}t} = D\frac{c_{res}}{x(t)} \qquad (4.2)$$

As the Stefan case is mathematically more simple and exhibits a well-defined reaction zone, some typical aspects of diffusion-limited processes shall be discussed on the basis of this model.

The initially very pronounced decrease of the reaction rate is typical for a diffusion-limited process. If high reaction-rates are intended, it is necessary to keep the length scale of diffusive transport as small as possible. This can be achieved by minimizing diffusion barriers inside the reservoir (e.g. by stirring). The diffusion barrier inside the medium can be minimized by working with small particles of the reactive medium. It must however be noted that the transport geometry in the case of small particles is different from that in the case of an extended medium. The same holds true for reaction geometries in which the reactant is provided from a spherical or an extended cylindrical source into the surrounding medium (inside-out-case). In fig. 8, the propagation speeds of the reaction zone in the 1D case and in the spherical and cylindrical cases are plotted as a function of the distance to the reaction zone both for "inside out" and "outside in" geometries. The most noteworthy difference between the different geometries is the asymmetry between the "inside-out" and "outside-in" case for the cylindrical and spherical geometries: In the first case, the reaction rates tend to decrease much faster in the case of the cylinder and even stronger for the sphere, while the reaction rate in the inside-out case is fastest for the sphere. Furthermore, the outside-in cases exhibit an increasing reaction speed shortly

before the innermost core of the sphere or the cylinder is reached and the material is completely saturated.

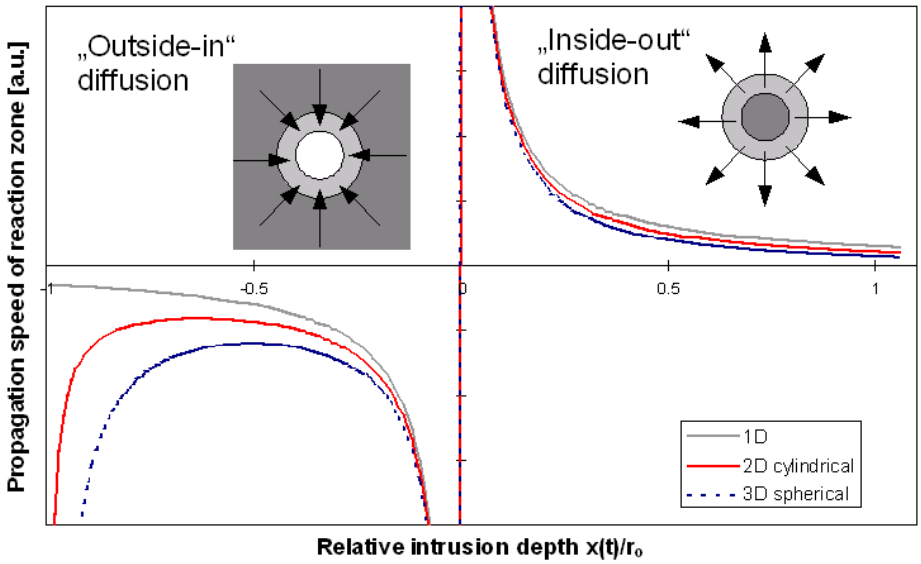


Fig. 8: Propagation speed of the reaction zone in a Stefan process. The “relative intrusion depth” in the case of the 1D geometry is normalized to the same length as the radius of the cylinder and the sphere. While the intrusion of the reaction zone in the 1D case is symmetrical, the intrusion of the reaction zone in the cylindrical and spherical geometries is different for the “outside in” and the “inside out” cases. The reason for this is the dependence of the radial volume element on the radius.

The reason for the differences between the geometries and the asymmetry between “outside-in” and “inside-out” diffusion cases is the volume element in the different geometries: In the cylindrical and in the spherical geometry, the volume element is given as

$$\mathrm{d}V_{cyl}(r) = 2\pi r\,\mathrm{d}r \text{ or } \mathrm{d}V_{sph}(r) = 4\pi r^2\,\mathrm{d}r\,.$$

This corresponds to a decreasing size of the volume element in the case of the outside-in geometry and an increasing size in the case of the inside-out geometry. As can be seen from figure 8, the decreasing volume element leads to an almost constant and finally even increasing traveling speed of the reaction zone inside the particle. Correspondingly, the growing volume element in an inside-out scenario leads to a progressive slowdown of the reaction front compared to the 1D case. Consequences of these geometry effects shall be discussed in sections 4.3, 4.4 and 4.8.

Despite the constant or even increasing propagation speed of the reaction front, one must be aware that the overall reaction rate nevertheless is decreasing with the intrusion of the reactant into the particles.

*4.2 Technical compromises in the design of particle-bed processes*

In order to achieve minimal losses in reactivity due to the diffusion-limitations just described, very small particles seem optimal for outside-in reactions such as ion exchange. However, handling very small particles often is inconvenient in the implementation of technical processes:

- The permeability of a particle bed dramatically decreases along with the particle size, furthermore, fine particle beds are more susceptible to clogging due to filtration effects,
- Keeping a fine particle bed together requires special filters at the exit of the column, otherwise particles might escape the column in suspension (and possibly do some mischief downstream),
- Fine particulate materials will require more precautions with respect to appropriate packaging and possibly also with respect to occupational health issues.

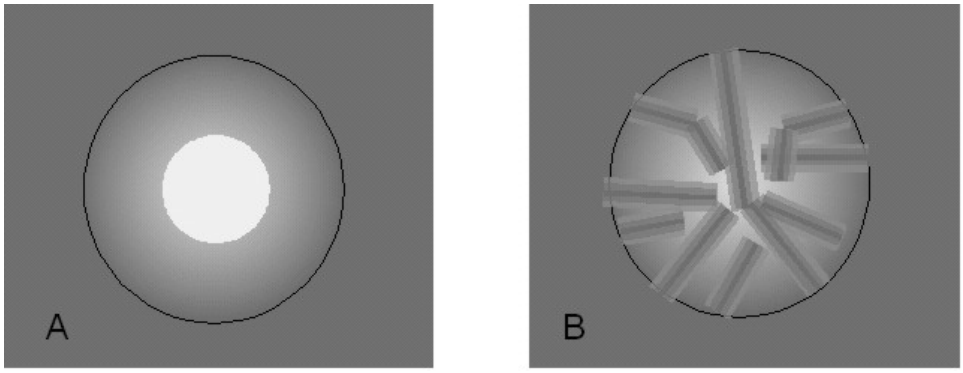


Fig. 9 Rough sketch of diffusive transport limitations (A) in a monolithic reactant bead (B) in a bead with internal porosity.

For a monolithic material, the best compromise will be choosing the smallest particle size which still can be reasonably handled. If the diffusion coefficient inside the particle material is much smaller than that in the surrounding medium, introducing additional porosity is a good option (see fig. 9): In this case, the actual diffusion length inside the active reaction medium is much shorter, and it is going to occur from channels with much faster diffusion inside. If the channels are filled by a free liquid phase such as water ($D = 2.3\times10^{-9}\mathrm{m}^2/\mathrm{s}$), the mean diffusive shift inside the channels will be on the order of a 1mm in a minute. Like that, a substantial diffusive material transfer from and to the active reaction medium can be achieved for a 2 mm diameter bead within a minute. If we assume a diffusion coefficient of $D = 2.3\times10^{-13}\mathrm{m}^2/\mathrm{s}$ for water inside the active material itself, a comparable diffusive material exchange would take 100 minutes, i.e. more than 1 hour.

While the porosity trick provides some remedy, it still doesn't solve the problem of diffusion limitation in general: increasing the particle diameter will still lead to increasingly strong diffusion limitations, and furthermore one must be aware that the

packing density of active material is decreased by introducing porosity. Nevertheless, particles with diameters on the mm scale and with some internal (macro-)porosity are a very common approach in the design of columns for applications as diverse as ion exchange and heterogeneous catalysis.

Basically, the design of optimal particles for column processes follows the rules:

- Minimize diffusive transport at low diffusion coefficient by introducing higher-diffusivity macroporosity,
- Keep diffusion-limited transport lengths at any diffusion coefficient as short as possible in order to fulfill other design requirements.

It must of course be stressed that the design of reactive columns is a very complex issue in research and technology and that diffusion effects are really just one issue among a multitude of others.

*4.3 Inside-out diffusion processes and controlled release*

While reaction columns typically are designed in order to provide a high reaction rate, there are other fields of technology where one is interested in a long-term and possibly constant release of some active agent. Examples are the release of active agents in pharmaceutical or agrochemical applications.

Applied in dissolved form or as a soluble, fine-grained material (such as the eosin dye in fig. 3), the active agent will be initially present at a very high concentration (which might actually be too high and poisonous) but readily be washed away or wasted by some decay reaction. This is not what we are interested in: Rather, we want to provide a moderate (and effective but not poisonous) concentration of the active agent over a long time. In this scenario (called controlled release), the slowing-down-effect of diffusion is actually a friend: However, the square-root-of-time effect and the geometry effects are again to be taken into account: Depending on the requirements of the application, the insertion of additional diffusion barriers (which might even be designed in a way that they slowly degrade along with the decreasing concentration of active agent), the use of slow-decaying precursor formulations or the observation of appropriate application schemes may be used in order to optimize the time-concentration profile achieved by the controlled release. Typical length scales in controlled release applications range from μm to mm. Nanoscale formulations are not of great interest for diffusion-controlled release as no sufficient delay by diffusion can be achieved in this case.

Nevertheless, nanoparticulate formulations are of great interest when it comes to poorly soluble active agents: here, the large surface area and the faster Brownian motion of smaller particles increase the distribution and the contact area of the agent in the system (leading to shorter distances the dissolved agent molecules have to travel in the water phase before reaching their sites of action). Furthermore, nanoparticles are capable of penetrating into biological cells. This latter aspect is presently a major challenge in research both for pharmaceutical technology and the study of possible health risks arising from nanoparticulate materials [22].

*4.4 Diffusive transport in organisms and biofilms*

The dimensions of biological cells are on a similar order of magnitude as mean diffusive shift of small molecules in aqueous media such as cytoplasm during a time of a second or less:

The length of individual bacteria is typically around 1 µm. At these dimensions, they do not need any active circulation systems (and circulation with Péclet numbers > 1 would require unrealistically fast flow inside the cells). Recently, giant bacteria with diameters up to 750 µm have been described [23]. In these bacteria, however, most of the cell volume is taken up by a large storage vacuole, and the metabolically active part of the bacterium is limited to a thickness of a few µm.

Large eukaryotic single-cell organisms such as *Paramecium* or *Noctiluca* very often measure several 100 µm or even more. This is already much larger than the mean diffusive shift of water during 1s. Such large single-cell organisms typically are equipped with at least some active intracellular transport mechanism for nutrients (for example, in the case of *Paramecium* it is possible to observe nutrient-filled vacuoles circulating through the organism).

In polycellular organisms, the need for active transport systems is even more obvious. Therefore, we find a wide range of different types of circulation and/or peristaltic systems inside all higher organisms. The tracheal system of insects combines the much faster diffusion of oxygen in the gas phase (with the finest tracheal openings penetrating into individual cells), some ventilation and an active pumping system for the nutrient-containing hemolymph. In vertebrates, both oxygen and nutrients are transported via the blood circulation. The vascular system again extends down to the cellular length scale so that diffusive transport is mainly limited to the sub-mm scale.

Understanding the mechanisms of vascular growth inside the human body is considered a key to novel therapeutic approaches to conditions such as coronary heart disease or cancer: Studies into the growth mechanisms of tumor tissues have indicated that solid tumors without an own vascular system can only reach sizes on the order of 1 mm [24]. In order to grow larger, the tumor needs to be connected to the blood stream by angiogenesis. Angiogenesis inhibitors such as bevacizumab [25] are in the progress of being introduced into the clinical therapy of cancer.

While polycellular organisms typically have at least some form of active transport systems that complements diffusive transport to larger length scales, some bacteria and other microorganisms go actually the other way and build some diffusion barriers around themselves. (In the case of a polycellular organism, the cells inside live in a cell-friendly environment so that their main concern is sufficient feeding. The environment for individual single-cell-organisms, by contrast tends to be a much rougher place so that protection against external hazards is at least as important as sufficient supply of nutrients.) The most frequent forms of diffusion barriers are gels consisting mainly of polysaccharides (so-called exopolysaccharides such as Xanthan or Gellan). While the exopolysaccharide layer forms only a minor diffusion barrier for dissolved oxygen or small nutrient molecules, the access of colloidal particles or predator microorganisms to the bacterium is strongly reduced.

Large and strong exopolysaccharide layers require a high metabolic investment from the respective microorganims. Due to the unfavourable inside-out-geometry, the amount

of material needed to form an exopolysaccharide layer around an individual bacterium is especially high. At the same time, the risk of damage such as partial dissolution of the gel barriers is also rather high for a free-floating microorganism.

A much more effective use of the exopolysaccharide barrier can be made by forming a biofilm: Sharing the gel barrier among many organisms will reduce the individual cell's metabolic investment in forming the barrier. Furthermore, the biofilm will lead to a quasi-one-dimensional diffusion geometry (with no-outside-in effect and thus with a smaller diffusive flow from the solution phase to the microorganism). Like that, the diffusion barrier formed by the exopolysaccharide has a mitigating effect on transient concentration highs of poisonous substances which will hit the microorganisms later and with a restricted peak value of its concentration.

Another aspect of moving together into a biofilm is the possibility of the microorganisms to form a "Verbund"-like community in which metabolites produced by one species may serve as nutrients for another microorganism present in the biofilm. Depending on their location and the organisms involved, biofilms can present a major problem (in medicine, hygiene and with respect to biofouling) or they are very useful (in some areas of biotechnology, e.g. for waste water treatment).

### *4.5 Diffusion in polymer technology*

Due to their large molecular weight, the diffusion coefficients of polymers are generally much lower than those of small molecules. This is even the case in dilute solutions. In more concentrated solutions or even more so in polymer melts, the translational movements of each polymer molecule are further restricted by the geometrical constraints exerted by the surrounding molecules. This effect is described by the reptation model of polymers and various refinements to it [26].

#### 4.5.1 Diffusion-limitations in polymerization processes: bulk, solution and emulsion polymerizations

In any case, diffusion coefficients in polymer melts tend to be quite low (well below $10^{-13}$ $m^2/s$) and also the viscosities of polymer melts are quite high. As a result, stirring concentrated solutions or melts of polymers is quite difficult, and diffusive mixing is very slow. While the diffusion coefficients for residual monomers are orders of magnitude higher than those of the polymer molecules, also their diffusion is strongly slowed down compared to a free liquid phase. Therefore, the diffusion limitation inside a polymerization batch becomes more and more of a problem with increasing degree of polymerization. In addition to material transport, also heat transport may be a serious issue as also the heat conductivity of polymer melts tends to be quite low and the high viscosities successfully suppress convective heat transfer, too.

Despite all these problems, many polymers still are produced in concentrated solutions (dilute solutions are unattractive as large quantities of solvent would have to be removed in order to recover the polymerization product) or in melts. For other polymers, however, emulsion polymerizations [27] have become more and more popular. In this process, the polymerization process is initiated inside amphiphilic micelles in a water phase. The monomers are provided in solution or as an emulsion . Monomer molecules diffusing from the water phase into the micelles with the growing polymer chains are

incorporated into the polymer chains. In the end, aqueous polymer dispersions [28] with solid contents of over 50% can be produced like that. In contrast to solution polymers and polymer melts, these dispersions exhibit moderate viscosities, and the final size of the polymer particles is about several 50 to several 100 nm in diameter. Over the length scales of such particles, diffusive transport is reasonably fast even for very low diffusion coefficients. The short length scales for intraparticle diffusion and the low viscosity of the dispersion allow easy mixing and heat transfer inside the polymerization batch. In contrast to bulk polymerization products, the resulting polymer dispersion contains large quantities of surfactants and other adjuvants. If dried above their respective minimum film formation temperature (MFFT), such dispersions will coalesce into continuous films. Depending on the properties of the polymer particles, the resulting films can be used for applications in paints, adhesives or paper and textile coating materials. In the film formation process, diffusion of polymer chains between individual particles may play some role; the main mechanism for the stabilization of the films is due to electrostatic and steric interaction forces between individual particles. Emulsion polymerizates can also be used for compounding into melts of other polymers (e.g. ABS where a synthetical rubber from an emulsion polymerisation process is mixed into an SAN melt).

4.5.2 Diffusive migration of small molecules in polymer materials

Other issues on diffusion in polymers include the diffusion of solvents, plasticizers, residual monomers or other small molecules through polymer matrices. Especially the possible diffusion of plasticizers and residual monomers from the polymer into surrounding phases creates great concern, especially in applications where the polymers are in contact with body fluids or food [29,30]. Diffusive migration of low-molecular weight species through polymers is not restricted to plasticizers or residual monomers: Small molecules may migrate through polymeric packaging materials. A demonstration for this effect can be seen from fig. 10 where two 10 ml aliquots of concentrated hydrochloric acid in a 10 ml polyethylene bottle (wall thickness 2.5 mm) and sealed into a 40 µm plastic bag were stored in closed tin containers for 1 day: While the container with the bottle is still intact, the container with the bag is already heavily corroded by HCl diffused through the polyethylene. In the case of the bottle, a comparable corrosion of the container wall was observed after about 100 days. The migration of oxygen through polymeric packaging materials is a major challenge in food packaging applications, for example polymeric bottles for beer (which is the common beverage most sensitive against oxygen diffusion [31]). A range of different approaches such as barrier layers [31,32], special coatings or oxygen-scavenging additives [33] in the polymers are used to overcome the oxygen-diffusion problem.

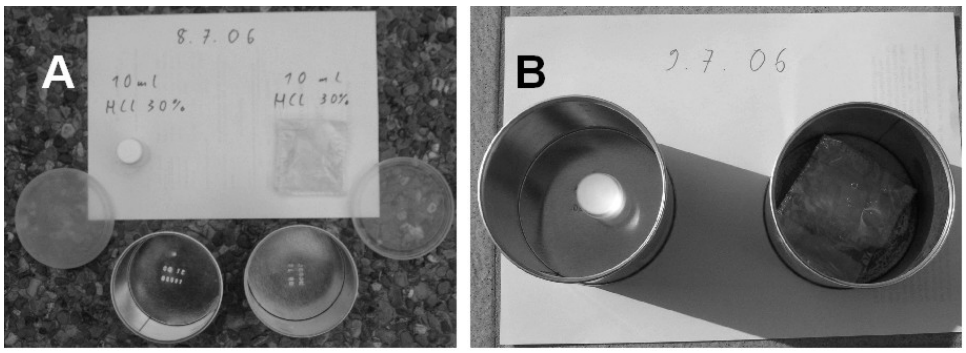

Fig. 10. Corrosion of a tin container by HCl diffusion through a PE bottle and a PE plastic bag: (A) both containers in intact state (B) situation after a day: while the walls of the container with the bottle are still clear, the container with the plastic bag is already heavily corroded.

Minimizing the diffusive ingress of oxygen and water vapour is an even more challenging task in the development of polymeric housings for polymeric or organic-molecule-based electronic devices such as Organic LEDs (OLEDs) which are highly sensitive to degradation by oxygen and water. Presently, only housings containing inorganic layers such as glass are capable of providing a sufficient diffusion barrier that allows a reasonable shelf and service life of such devices. Flexible devices may be realized by polymer-reinforced ultrathin glass layers [34].

*4.6 Diffusion in functional materials for electronics*

Diffusion is not just a challenge in organic electronics, but also in the production and performance of classical devices such as semiconductor electronics or batteries. With some exceptions such as ion-conducting materials, (chemical) diffusion coefficients in crystalline solids tend to be very low[1]. For example, the diffusion coefficients of doping atoms such as P or As in Si are about $10^{-18}m^2/s$ at temperatures around 1000°C. This corresponds to mean diffusive shifts in the sub-µm range during a 30-min tempering episode at 1000°C [35]. Extrapolating empirical findings on the temperature dependence of dopant diffusion in Si [36] down to room temperature, we arrive at diffusion coefficients around $10^{-48}m^2/s$ which would correspond to a mean diffusive shift of 1 nm after $10^{22}$ years! However, it should be noted that other atomic species such as for example Cu exhibit much higher diffusion coefficients in solid Si or $SiO_2$ barrier materials and therefore may already lead to rapid diffusive degradation of microelectronic devices at temperatures around 300 °C or lower [37].

[1] It should be noted that there are also charge carrier diffusion processes taking place in solids. For example, diffusion currents of electrons and holes are responsible for the specific current transport properties of semiconductor p-n-junctions (diodes). The diffusion of the charged quasiparticles can be described by means of the Nernst-Planck-Equation (see 4.6.2).

4.6.1 Semiconductor nanostructures: stability and growth

The high activation energies of diffusion in semiconductors explain why it is possible to produce devices with dopant profiles at nm-resolution and nevertheless have completely stable structures at room temperature for "infinitely" long times. It also explains why the development of high-temperature electronics presents special material challenges.

By appropriate growing techniques such as molecular beam epitaxy (MBE) it is possible to realize high-quality multilayer structures of different semiconductor materials at "atomic" resolution. A major reason why these techniques actually work is the dramatic difference between the diffusion coefficient of ad-atoms on the surface and the diffusion of atoms in already complete layers [38]. Due to the temperature dependence of both the inter-layer diffusion and the diffusion of ad-atoms, the choice of the substrate temperature plays a key role in controlling MBE growth. Further improvements in controlling diffusion between the layers can be achieved by introducing special diffusion barrier layers [39].

4.6.2 Battery materials: long-term stability despite high diffusion coefficients

In charged primary and secondary batteries, the two electrodes are separated by an ion-conducting liquid, polymeric or solid layer. In fig. 11, a schematic representation of a cell for a lithium battery is given. In commercial lithium batteries, the thickness of the individual cells is on the order of a few 100 µm, and they are stacked or scrolled together to squeeze as much as possible storage capacity inside the battery housing. The space left for the separator inside such cells is on the order of 100 µm or less.

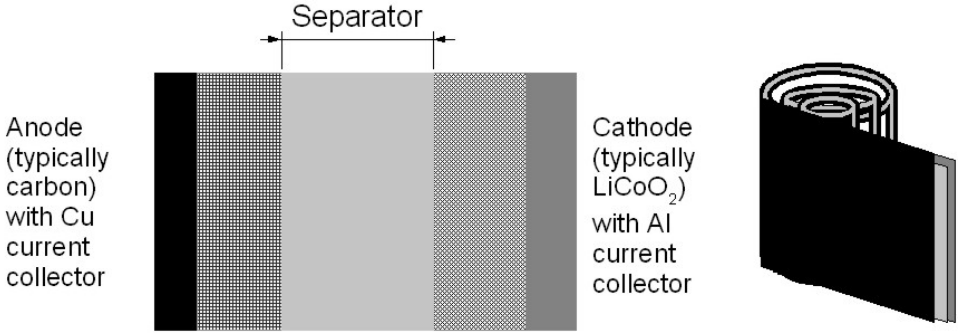


Fig. 11. Layout of film electrodes and separator in a Li ion battery. The overall layers structures are just a few 100 µm thick and are scrolled together into the battery housing.

Present separators consist of lithium-conducting polymers, gels or porous materials soaked with a non-aqueous solution of a Li salt such as $LiPF_6$. In order to be good ion conductors for $Li^+$ (which is needed in order to achieve a low internal resistance of the battery), these systems are characterized by high mobilities of the $Li^+$ ions. This $Li^+$ mobility is not only reflected in the ionic conductivities but also in self-diffusion coefficients of $Li^+$ ions that may range around several $10^{-10}$ $m^2/s$ [40]. Such diffusion coefficients correspond to a mean diffusive shift of 100 µm in roughly a minute. Therefore it may seem likely that such a battery should self-discharge as a matter of minutes. However, state-of-the-art lithium batteries have self-discharge times of several months. The reason for this seemingly paradox stability is the charged nature of the $Li^+$

ions: the diffusive propagation of $Li^+$ ions without appropriate counterions is suppressed by the buildup of strong local electric fields. The description of the diffusion of ions therefore needs a modified form of Fick's first law which is known as the Nernst-Planck equation:

$$j_i = -D_i\left(\frac{\mathrm{d}c_i}{\mathrm{d}x} + z_i c_i \frac{F}{RT}\frac{\mathrm{d}\Phi}{\mathrm{d}x}\right). \qquad (4.3)$$

The diffusion of different ionic species $i$ with electrical charge $z_i$ is coupled together by the derivative of the electric potential $\Phi$. ($R$ denotes the general gas constant, $F$ the Faraday constant and $T$ the temperature.)

In the case of the charged battery, the absence of counterions capable of diffusion through the separator leads to a stabilization of the non-equilibrium distribution of the $Li^+$ ions despite the absence of diffusion barriers.

*4.7 Diffusive mixing in microfluidics*

Microfluidic systems are increasingly used in chemical research labs ("lab on a chip", high-throughput screening, …) and the first industrial applications of microreactors for production purposes have also been presented [41,42,43]. Due to the short distances between the active surfaces and the "bulk liquid" in typical channels (5 to 100 µm diameter), diffusion often provides sufficiently good mixing of the reactants so that no further active mixing measures have to be taken [41]. In systems with high flow velocities (several mm/s or higher), diffusive mixing still can take several seconds which correspond to channel lengths of several cm [44]. If such long channels are not desired or if fast reaction kinetics dictate faster mixing time, mixing has to be sped up. A range of active mixing devices such as miniaturized magnetic stir bars [45], paramagnetic flagellae driven by rotating magnetic fields [46], miniaturized peristaltic pumps [47] or particles operated by optical traps [48] have been suggested and demonstrated. The essential effect of all these devices is that they are supposed to reduce the length scale for diffusive mixing even further down as mixing times (and such needed flow path lengths) will decrease with the square of the remaining length scale. Active mixing devices are often difficult to produce by established microstructuring techniques and they need additional infrastructure such as magnetic fields or laser beams for operation. Therefore, passive mixing techniques aiming at creating cross-flows between the individual laminae of the liquid inside the channels are considered a much easier way to enhance mixing performance in microfluidic devices [49] or the introduction of porous structures with well-defined tortuosity properties inside the microfluidic channels [44].

*4.8 Heat transfer at micro- and macroscales*

Heat transfer processes on the macroscopic scale are present in many aspects of everyday life: Heat conduction through house walls, cooking and heat management in chemical process technology are just a few examples. In most of these situations, we're dealing with instationary heat transfer processes. In this case, not just the heat conductivity $\lambda$ but also the heat diffusion coefficient $\alpha$ is relevant for the heat propagation process: While the heat conductivity describes the heat current through a wall during stationary conditions, the heat diffusion coefficient is relevant for the propagation of a

temperature variation through the wall. Two walls with the same heat current under stationary conditions (e.g. a wooden wall with $\lambda = 0.13\ Wm^{-1}K^{-1}$ and 5 cm thick and a stone wall with $\lambda = 2.6\ Wm^{-1}K^{-1}$ and 1 m thick) will not necessarily take the same time to heat up: In the case of the wooden wall (heat diffusion coefficient $1.1\times10^{-7}m^2/s$), it takes roughly 3 hours for half of the temperature difference to arrive at the inner side of the wall. In the case of the stone wall (heat diffusion coefficient $1.1\times10^{-6}m^2/s$), it takes roughly 6 hours for half of the temperature difference to arrive at the inner side of the wall. This difference is mirrored in traditional house construction schemes in different parts of the world: In arctic regions throughout the word, we find relatively thin wooden walls, while thick stone or clay walls are common in regions with dry and hot summers and high temperature variations during the day such as Mediterranean or the Middle East. In such houses, daytime high temperatures will take a very long time to migrate through the wall, and it is possible to keep the house much cooler than the outside high temperatures over quite long times. In the arctic, by contrast, warm daytime temperatures are rather welcome in the house and so the rather fast heat diffusion through the wall actually proves advantageous.

In cooking, a uniform heating of the pot's content is desired. In low-viscosity liquids such as water or oil this can be achieved without further measures due to the formation of density-driven convection rolls. In higher-viscosity food systems such as thickened sauces or for interstitial water between solid foodstuffs such as noodles, the formation of convection rolls is suppressed and active stirring is necessary to avoid overheating (and subsequent sticking to the pot) near the bottom of the pot at high heating rates. At lower heating rates, no sticking will occur but heating up all the food by just heat conduction may take very long time and the cooking times in the pot will be unevenly distributed. For extended solid materials such as pieces of meat, heating the inside to the required cooking temperature is either realized by frying (i.e. a high heating rate and much higher temperatures reached at the outside) or by boiling at constant temperature in water. The frying time needed for pieces of different thickness increases again with the square of the pieces' thickness. Furthermore, the resulting texture of the fried food will vary much stronger with depth inside a thick piece than inside a thin one. Thermally instable (yet nutrionally valuable) components of the food may be degraded due to long periods at elevated temperatures during heating and cooling of large batches of food. A common example for this is ultrahightemperature (UHT) processing of milk (several seconds at temperatures up to 150 °C) which is nearly as effective as sterilization (several minutes at 121 °C, heating inside the whole bottles) for achieving long shelf life at room temperature. Heating and cooling a small quantity of the milk to 150 °C leads to much smaller losses in micronutrients than the sterilization process in which long heating and cooling times have to be considered along with the duration of the actual high-temperature treatment.

Similar effects are also found in the handling of biotechnological products which may need very fast cooling as a first step to product recovery. When just mixing a cell slurry with ice water for cooling, heat diffusion processes inside the material may lead to partial degradation of the desired products. Cooling the cell suspension in microfluidic heat exchanger systems can avoid much of these problems [50].

Finally, heat management in chemical reactions depends a lot on the dimensions of the reactor system: In a sufficiently thick structure, even a moderate exothermic effect such as the heat release by hydrating cement may lead to substantial heating (massive concrete structures may easily reach temperatures of 80°C inside during the first days of hydration; in order to minimize this problem, special, slow-hydrating concrete mixtures may be used for such structures). In the case of more exothermic reactions, much more dramatic heating may occur and often must be avoided in order to prevent a catastrophic further heating of the reaction system. The most simple approach to active heat management is again stirring which might be complemented by the introduction of heat exchanger systems inside the reactor. Adjusting heating and cooling in a reactor system is one of the challenges that need to be addressed in scaling up a process from conventional lab size or production plant size. In the chemical industry, this is often done with experiments in miniplants as an intermediate stage.

With the advent of microreactor systems, another option for heat management has become available: here, only very short distances need to be traveled by heat conduction through the reacting mixture, and furthermore, the conductive heat transfer through the reactor housing roughly corresponds to a cylindrical "inside-out" heat conduction scenario. Stacks of microreactors instead of one large-scale reactor will provide an option for easier heat management even at production scale in the future (at least for some products), and the problematic scaling up process with changing conditions for heat-management may come down to a simple "numbering up" [51].

## 5 Conclusion

As the different examples in the last chapter show, the square-root-of-time scaling behaviour of both energy and particle diffusion leads to considerable differences in transport processes at different length scales. Understanding and controlling the role of diffusion processes for transport at small length scales is a fascinating challenge in many fields of science ranging from basic physics to chemical engineering, medicine and even food science and civil engineering. Research into diffusion therefore provides an important basis for sustainable technological development.

## References


[1] A. Lachke, Resonance 9/10 (2004), 25-33.
[2] J. Philibert, Diffusion Fundamentals 4 (2006) 6.1 - 6.19.
[3] W. Simpson, A. TenWolde, in: Forest Products Laboratory, Wood Handbook, FPL-GTR-113, Madison WI, 1999, pp. 3-1 - 3-25.
[4] H.S. Carslaw, J.C. Jaeger, Conduction of Heat in Solids, Clarendon Press, Oxford, 1959.
[5] J. Crank, The Mathematics of Diffusion, Clarendon Press, Oxford, 1975.
[6] E. Péclet. Traité de la Chaleur Considerée dans ses Applications, vol. 3. Hachette, Paris, 1843.
[7] J. Clerk Maxwell, Phil. Trans. Royal Soc. London 157 (1867) 49-88.
[8] A. Einstein, Investigations on the Theory of the Brownian Movement, edited with notes by R. Fürth, Dover publications, New-York, 1956.

[9] M. von Smoluchowski, Annalen der Physik, 4. Folge, 21 (1906) 756-780
[10] G. Hevesy, A Manual of Radioactivity, Oxford University Press, 1938.
[11] E.O. Stejskal, J.E. Tanner, Journal of Chemical Physics 42 (1965) 288-292.
[12] F. Stallmach, P. Galvosas, Spin echo NMR diffusion studies Annu. Rep. NMR Spectrosc 61 (2007) 51-131.
[13] A. Gädke, N. Nestle, Diffusion Fundamentals 3 (2005) 38.1 - 38.12.
[14] J.E. Tanner, Journal of Chemical Physics 52 (1970) 2523-2526.
[15] P.T. Callaghan, Principles of Magnetic Resonance Microscopy. Clarendon Press, Oxford, 1991.
[16] N. Nestle, P. Galvosas, J. Kärger, Cement and Concrete Research 37 (2007) 398-413.
[17] N. Nestle, A. Qadan, P. Galvosas, W. Süss, J. Kärger, Magnetic Resonance Imaging 20 (2002) 567-573.
[18] S. Vasenkov, P. Galvosas, O. Geier, N. Nestle, F. Stallmach, J. Kärger, Journal of Magnetic Resonance 149 (2001) 228–233.
[19] J. Stefan, Wiedemanns Annalen der Physik und Chemie, 3.Folge 42 (1891) 269-286.
[20] N. Nestle, R. Kimmich, Biotechnology and Bioengineering 51 (1996) 538-543.
[21] N. Nestle, R. Kimmich, Heat and Mass Transfer (Wärme- und Stoffübertragung) 32 (1996) 9-15.
[22] P.H.M. Hoet, I. Brüske-Hohlfeld, O.V. Salata, Journal of Nanobiotechnology 2 (2004) 12, http://www.jnanobiotechnology.com/content/2/1/12
[23] H.N. Schulz, T. Brinkhoff, T.G. Ferdelman, M. Hernandez Mariné, A. Teske, B.B. Jorgensen, Science 284 (1999) 493-495.
[24] J. Folkman, Ann. Surg. 175 (1972), 409-416..
[25] S.D. Zondor, P.J. Medina, Ann Pharmacother. 38 (2004) 1258-1264.
[26] M. Doi, S.F. Edwards, 1986 Theory of Polymer Dynamics, Academic Press, New York, 1986..
[27] U. S. Patent 1732795, filed Sept.13, 1927.
[28] D. Urban, K. Takamura, Polymer Dispersions and Their Industrial Applications, VCH, Weinheim, 2003.
[29] EU COMMISSION DIRECTIVE 2002/72/EC
[30] T. Begley et al., Food Additives & Contaminants, 22 (2005) 73 – 90.
[31] N. Boutroy et al., Diamond & Related Materials 15 (2006) 921 – 927.
[32] J. Lange, Y. Wyser, Packaging Technology and Science, 16 (2003) 149 – 158.
[33] A. López-Rubio, E. Almenar, P. Hernandez-Muñoz, J. M. Lagarón, R. Catalá, R. Gavara, Food Reviews International, 20 (2004) 357-387.
[34] K.S.Ong, J.Q.J.Hu, R.Shrestha, F.R.Zhu, S.J.Chua, Thin Solid Films, 477 (2005) 32-37.
[35] S. Eguchi, J.L. Hoyt, C.W. Leitz, E.A. Fitzgerald, Appl. Phys. Lett., 80 (2002) 1743-1745.
[36] M.R.Murti, K.V.Reddy: Semiconductor Science and Technology, 1989, 4, 622-5
[37] S.H. Tey, K. Prasad, K.C. Tee, L.H. Chan, E.G. Seebauer, Thin Solid Films 466 (2004) 217–224.

[38] J.S. Song, S.H. Seo, M.H. Oh, J.H. Chang, M.W. Cho, T. Yao, Journal of Crystal Growth 261 (2004) 159–163.
[39] N. Jin, et al., Materials Science in Semiconductor Processing, 8 (2005) 411–416
[40] Y. Aihara, T. Bando, H. Nakagawa, H. Yoshida, K. Hayamizu, E. Akiba, W.S. Price, Journal of The Electrochemical Society, 151 (2004) A119-A122.
[41] W. Ehrfeld, V. Hessel, V. Haverkamp, Microreactors in: Ullmann's Encyclopedia of Industrial Chemistry, 6th Edition, VCH, Weinhein (1999).
[42] K. Jähnisch, V. Hessel, H. Löwe, M. Baerns, Angew Chem Int Ed Engl., 43 (2004) 406-446.
[43] D. Kirschneck, G. Tekautz, Chemical Engineering and Technology, 30 (2007) 305-308.
[44] S. Jeon, V. Malyarchuk, J.O. White, J.A. Rogers, Nano Letters 5 (2005) 1351-1356.
[45] L. Lu, K. Ryu, C.J. Liu, Microelectromech. Syst. 11 (2002) 462-469.
[46] S. L. Biswal, A. P. Gast, Anal. Chem. 76 (2004) 6448-6455.
[47] M. Oddy, J. Santiago, J. Mikkelsen, Anal. Chem. 73 (2001) 5822-5832.
[48] A. Terray, J. Oakey, D. Marr, Science 296 (2002) 1841-1844.
[49] R. Liu, M. Stremler, K. Sharp, M. Olsen, J. Santiago, R. Adrian, H. Arl, D.J. Beebe, Microelectromedh. Syst. 9 (2000) 190-197.
[50] C. Wiendahl, J. J. Brandner, C. Küppers, B. Luo, U. Schygulla, T. Noll, M. Oldiges Chem. Eng. Technol. 2007, 30 (2007) 322–328.
[51] W. Ehrfeld, V. Hessel, H. Löwe, Microreactors, VCH, Weinheim, 2004.